

1 **Title page**

2

3 **A machine-learning method based on ocular surface features for COVID-19**
4 **screening**

5 Feng Li^{1*}, Xiangyang Xue^{2,3*}, Qiang Sun⁴, Haicheng Tang¹, Wenxuan Wang³, Mengwei
6 Gu^{2,5#}, Yanwei Fu^{2#}

7

8 **Affiliations**

9 1, Department of Critical Care Medicine, Shanghai Public Health Clinical Center, Fudan
10 University, Shanghai, 201508, China

11 2, School of Data Science, Fudan University, Shanghai, 200433, China

12 3, School of Computer Science, Fudan University, Shanghai, 200433, China

13 4, Academy for Engineering & Technology, Fudan University, Shanghai, 200433, China

14 5, AIMOMICS INC., KY1-1104, CYM

15

16 * These authors contribute equally to this study.

17 # Corresponding author: Mengwei Gu (michael0990@aliyun.com) and Yanwei Fu
18 (yanweifu@fudan.edu.cn).

19

20

21 **Short title:** An ocular surface feature-based method for COVID-19 screening.

22

23

24 **Abstract**

25 **Background**

26 The standard practices for screening patients with COVID-19 are the CT imaging or
27 RT-PCR (real-time polymerase chain reaction) for testing viral nucleic acid, which is
28 expensive and in need of professional equipment and waiting time.

29 **Methods**

30 Literatures have shown that the COVID-19 patients are usually accompanied by ocular
31 manifestations. We constructed a machine-learning model based on ocular surface
32 features and proposed a new screening method for COVID-19. A retrospective study of
33 analyzing 446 subjects and a prospective study with 128 subjects were conducted with
34 this method. The performance was measured at receiver-operating-characteristic curve
35 (AUC), sensitivity, specificity and accuracy.

36 **Results**

37 The performance of detecting COVID-19 patients in the retrospective study have achieved
38 an AUC of 0.999 (95% CI, 0.997-1.000), with a sensitivity of 0.982 (95% CI, 0.954-1.000),
39 and a specificity of 0.978 (95% CI, 0.961-0.995). And in the prospective study, our model
40 performance on COVID-19 has achieved an AUC of 0.980 (95% CI, 0.970-0.990), with a
41 sensitivity of 0.770 (95% CI, 0.694-0.846), and a specificity of 0.973(95% CI,
42 0.957-0.989).

43 **Conclusion**

44 This deep learning method based on eye-region images demonstrates the high accuracy
45 to distinguish COVID-19 patients. We hope this study can be inspiring and helpful for
46 encouraging more researches on this topic.

47

48 **Keywords** COVID-19, ocular surface feature, deep-learning, screening

49

50

51 **Introduction**

52 The Coronavirus disease 2019 (COVID-19) pandemic has caused more than one million
53 deaths¹ since first breakout. Fever is one of the typical symptoms of COVID-19 patients,
54 with a range of 43.8%² to 98%^{3,4}. Accordingly, body temperature has been the initial and
55 most widely used screening method for COVID-19 patients⁵. Meanwhile, the emergence
56 and rising number of asymptomatic COVID-19 patients⁶ are posing a threat to body
57 temperature based screening method. Hence, developing other COVID-19 screening
58 methods is of urgent needs.

59 In recent years, artificial intelligence (AI) has achieved remarkable performance in
60 computer vision and medical analysis, including chest computed tomography (CT) based
61 AI system for COVID-19 diagnosis^{7,8}, and ocular diseases like diabetic retinopathy and
62 glaucoma⁹. Notably, SARS-CoV-2 has been detected from COVID-19 patients' ocular
63 secretions¹⁰, and extrapulmonary manifestations¹¹, including ocular symptoms
64 (conjunctival congestion, sagging eyelids, etc.^{12,13}) were reported for COVID-19 patients,
65 which inspires us to develop an AI model to screen COVID-19 patients, only based on
66 ocular surface images captured by common CCD cameras.

67 In this study, we constructed a machine-learning model based on ocular surface features,
68 and conducted a retro-prospective study to screen asymptomatic/mild COVID-19 patients
69 from healthy volunteers, pulmonary disease patients without COVID-19 (e.g., pulmonary
70 fungal infection, bronchopneumonia, chronic obstructive pulmonary disease, and lung
71 cancer) , and ocular disease patients. The results reveal that asymptomatic/mild
72 COVID-19 patients have distinguished ocular features from others. The convenient
73 method would provide an alternative choice for asymptomatic/mild COVID-19 patients
74 screening and guide effective prevention and control measures against COVID-19.

75

76

77

78 **Methods**

79 ***Study design and oversight***

80 We conducted a retro-prospective training, validation and testing study on a deep learning
81 model using ocular surface photos to screen COVID-19 patients (**Figure 1**). This study
82 included 2,108 photographs from 569 participants (retrospective 446 and prospective 123)
83 which included healthy volunteers, COVID-19 patients, pulmonary diseases or ocular
84 diseases. All 1561 photographs in the open-labeled retrospective study were used for
85 model training and validation, and 547 photographs in the single-blind (to AI group)
86 prospective study were used for testing. The study was conducted in accordance with the
87 principles of the Declaration of Helsinki. This study was approved by the Ethics
88 Committee of Shanghai Public Health Clinical Center (approval No.: YJ-2020-S078-02),
89 and informed consents have been obtained.

90 ***Study subjects***

91 The participants were enrolled from Shanghai Public Health Clinical Center (SPHCC),
92 Fudan University. In the retrospective study, 143 healthy volunteers, 104 COVID-19
93 patients, 131 pulmonary disease patients, and 68 ocular patients were included, from
94 2020 April 1st to June 30th. The prospective study comprises 35 healthy volunteers, 29
95 COVID-19 patients, 31 pulmonary and 33 ocular diseases patients, from 2020 July 1st to
96 August 31st (**table 1**). Of 133 COVID-19 patients, 47 (retrospective 24 and prospective 23)
97 were asymptomatic/mild type. Most of the COVID-19 are with a from East Asia (87.50%
98 and 93.10%) for retrospective and prospective studies. The demographic and clinical
99 characteristics of COVID-19 patients were shown in **table 2**.

100 **Definition of participants**

101 The COVID-19 patients were confirmed by the RT-PCR detection for viral nucleic acids.
102 According to the eighth version guideline published by the National Health Commission of
103 China, asymptomatic COVID-19 carriers refers to individuals with viral nucleic acid test
104 positive, and no clinical symptoms and no signs of pneumonia in chest imaging. The
105 patients with pulmonary diseases other than COVID-19 were diagnosed as
106 bronchopneumonia, chronic obstructive pulmonary diseases, pulmonary fungal infection
107 and lung cancer, etc. The patients with ocular diseases were diagnosed as trachoma,
108 pinkeye, conjunctivitis, glaucoma, cataract and keratitis, etc. The healthy volunteers were
109 collected from individuals who had taken physical examination and no obviously abnormal
110 results were demonstrated. All the subjects were tested for the COVID-19, and no
111 participants showed viral nucleic acids positive during the following days, except for
112 COVID-19 patients. No death events were observed in this study.

113 ***Image acquisition and exclusion***

114 For each participant, 3-5 photographs of the ocular surface were taken using the common
115 CCD and CMOS cameras, assisted by doctors or healthcare workers. The same shooting

116 plain mode and parameters were used, and avoid shooting filters. The photos were
117 captured in a good lighting condition, and not in dark or red background. The image
118 resolution is at least 1900x500 96dpi. A total of 609 photographs (retrospective 447 and
119 prospective 162) were taken from healthy volunteers, 506 photographs (retrospective 367
120 and prospective 139) from COVID-19 patients, 589 photographs (retrospective 473 and
121 prospective 116) from pulmonary and 404 photographs (retrospective 274 and
122 prospective 130) from ocular disease patients. 27 (retrospective 6 and prospective 2)
123 photographs from 8 participants with low quality were excluded.

124 ***Developing the deep-learning classification***

125 The schematic of our proposed DLS is illustrated in **Figure 2**, which consists of two
126 components, the Image Preprocessing¹⁴ and Classification Network^{15,16}. Specifically, the
127 Image Preprocessing receives raw ocular images, and prepare them for model training or
128 inference. For the Classification Network, it studies the characteristics of ocular surfaces
129 according to the inputs, and learns texture and semantic embeddings. Finally, the risk
130 assessment of pneumonia (i.e., Healthy volunteers, COVID-19, pulmonary and ocular
131 disease patients) is performed by a classifier with the extracted features.

132 The Classification Network is trained on the training data, and evaluated on the testing
133 and validation data. The testing and validation data is are not used to train the network.
134 Particularly, we apply five-fold cross-validation¹⁷ in the retrospective study, where all the
135 retrospective samples are randomly partitioned into five equal sized subsets. Of the five
136 subsets, a single subset is retained as the data for testing the model, and the remaining 4
137 subsets are used as training and validation data. The cross-validation process is then
138 repeated five times, with each of the five subsets used exactly once as the testing data. In
139 the prospective study, all the training and validation data are used for model training, and
140 the performance of deep learning is measured at the test dataset.

141 Considering that the subjects may provide more than one image in the realistic test, we
142 should classify them based on the prediction results of multiple images¹⁸. Therefore, we
143 conduct the risk screening for subject based on the previous image-level predictions and
144 set the priority, e.g., the COVID-19 is the most emergency situation, next is pulmonary,
145 then ocular, and the last is healthy category. In other words, if one of the multiple images
146 belonging to a person is predicted with the COVID-19, we assume that that person is most
147 likely to be a patient with COVID-19.

148 ***Statistical analysis***

149 To measure the performance characteristics, we used the one-versus-rest and
150 COVID-19-versus-other strategy and calculated the area under the
151 receiver-operating-characteristic curve (AUC), sensitivity, specificity, and accuracy
152 according to the results of our classification model. Bootstrapping was used to estimate 95%
153 confidence intervals of the performance metrics, with the photo as the resampling unit.

154 The One-vs.-Rest setting refers to splitting the disease classification task into one binary
155 classification problem per class; and the COVID-19-vs.-One setting means classifying one
156 binary classification problem into either COVID-19, or another disease.

157

158 **Results**

159 **Retrospective classification performance of COVID-19**

160 In the retrospective study, we first conduct the 5-fold cross-validation on the training and
161 validation datasets. All data is randomly partitioned into five equal sized subsets, and
162 there is no identity overlap among the subsets. Of the five subsets, one subset is utilized
163 as the testing data, and the remaining four subsets are used for training the model. The
164 cross-validation process is then repeated five times, with each of the subset used exactly
165 once as the testing data. Bootstrap is used to estimate the confidence interval for each
166 model. Then the five results can be averaged to produce a single average estimation. In
167 the One-vs.-Rest setting, the average AUC of COVID-19 -vs.-Rest is 0.999 (95%CI,
168 0.997-1.000). The sensitivity and specificity of COVID-19-vs.-Rest is 0.982 and 0.978
169 respectively. In the Covid19-vs.-One setting, the AUC is 0.999 (95% CI, 0.998-1.000),
170 0.997(95% CI, 0.993-1.000), 1.000 (95% CI, 1.000-1.000) with respect to health
171 volunteers, pulmonary and ocular diseases (**Table 3** and **Figure 3**).

172 **Prospective classification performance of COVID-19 patients**

173 In the prospective study, we tested the performance on the test set in both One-vs.-Rest
174 and COVID-19-vs.-one setting. Particularly, we investigate whether the model can
175 distinguish the asymptomatic/mild COVID-19 patients from other groups of subjects. In
176 the One-vs.-Rest setting, the average AUC of COVID-vs.-Rest is 0.980 (95%CI,
177 0.970-0.990). The sensitivity and specificity of COVID-vs.-Rest is 0.770 and 0.973,
178 respectively. In the COVID-19-vs.-One setting, the AUC is 0.963 (95% CI, 0.944-0.982),
179 1.000 (95% CI, 1.000 -1.000), 0.998 (95% CI, 0.996-1.000) with respect to health
180 volunteers, pulmonary and ocular diseases. Particularly, the AUC of COVID-19
181 (asymptomatic/mild)-vs.-one is 0.960 (95% CI, 0.939-0.981), 1.000(95% CI, 1.000 -1.000),
182 0.999 (95% CI, 0.997-1.000) with respect to health volunteers, pulmonary and ocular
183 diseases (**Table 4** and **Figure 4**). The results of COVID-19(asymptomatic/mild)-vs.-one
184 are close to COVID-19-vs-one. The 0.003 decrease on the AUC of distinguishing from
185 health volunteers, means it is harder to distinguish the asymptomatic/mild COVID-19
186 patients from health volunteers.

187 The overall classification system performed well, misjudgment also appeared. In the
188 prospective study, the 139 photos of COVID-19 patients have 107 classified correctly, 30
189 misclassified as health volunteers, and 2 misclassified as pulmonary patients. The 162
190 healthy people have 150 classified correctly, 2 misclassified as ocular disease and 10
191 misclassified as COVID-19 where 8 photos belong to the patients who just turned into

192 COVID-19 negative from positive. In reality, one person can take multiple photos as the
193 input of the model, which can strengthen the robustness of the model, which is widely
194 used in ensemble learning. With a privilege voting strategy, we can boost the sensitivity
195 performance of the model on the most important disease. As a result, only 1 COVID-19
196 patient was misclassified as health volunteers, 28 were classified correctly in the
197 prospective study. The confusion matrix of classification results of subjects on the
198 retrospective and prospective study were shown in **Figure 5**.

199 **Ablation study on full eyes, left eye and right eye**

200 Since the eyes are symmetrical, we conduct an ablation study to investigate whether the
201 left or right eye contain more information for medical diagnosis. **Table 6** shows that the
202 model with the right eye as input is best on the accuracy in the classification of health
203 volunteers, COVID-19, pulmonary and ocular patients. The model with full eyes is better
204 than the model with the left eye on COVID-19, pulmonary and ocular patients.

205 **The continuous observations of patients who turn into COVID-19 negative**

206 At last, we made a continuous observation of 4 patients turning from COVID-19 positive to
207 negative. As shown in **Table 7**, when turned into COVID-19 negative the four patients are
208 less likely ($8/15 = 53.3\%$) to be diagnosed as COVID-19 than the time when they are
209 COVID-19 positive ($12/16 = 75.0\%$), but still has a much more chance to be misclassified
210 as COVID-19 patients than the normal healthy people who only has the possibility
211 ($2/147=1.4\%$) to be misclassified as COVID-19 patients.

212

213

214

215 **Discussion**

216 Detecting abnormal body temperature has been the initial and most widely used
217 screening method for COVID-19 patients. Meanwhile, the emergence and rising number
218 of asymptomatic COVID-19 patients are posing a threat to body temperature based
219 screening method. On one hand, despite the high sensitivity and good specificity of
220 detecting the nucleic acid sequence of pathogens and amplify the signal by amplification
221 reaction, the long process of RT-PCR may remarkably increase the risk of infection, less
222 ideal for the epidemic control. On the other hand, conventional CT tests can show that
223 patients with COVID-19 can have bilateral ground-glass appearance and pulmonary
224 turbidity, analyzed by radiologists, or deep learning algorithms, however, for some patients,
225 CT imaging results are not obvious or even negative. Particularly, there are many other
226 bottlenecks and difficulties for the COVID-19 diagnosis globally, such as the restriction of
227 pharyngeal swab sampling, the lack of RT-PCR kits, the difficulties in the transportation,
228 the preservation of samples, political factors in some country, and so on.

229 Our model can successfully classify COVID-19 patients from healthy persons, pulmonary
230 patients except for COVID-19 (e.g., pulmonary fungal infection, bronchopneumonia,
231 chronic obstructive pulmonary disease, and lung cancer) , and ocular patients. The model
232 has two major components: an image preprocessing method to detect, crop and align the
233 eye area from the input image, and a deep learning based classification network to extract
234 discriminative features and recognize COVID-19 patients based on the processed
235 eye-region data. The ocular surface features extracted by DL model from the training data
236 show that the eye features of different diseases have obvious differences and have
237 certain regularity. For healthy person, the DL model extract the ocular surface features
238 around the iris, sclera and eyelid through the healthy people. To sum up, after eliminating
239 the influence of human eye pose and iris position, we have the following conclusion that,
240 (1) The DL model extracted features to healthy people is mainly focused on iris, with
241 evenly distributed features; (2)The model's attention to non-COVID-19 pneumonia
242 patients is mainly concentrated near the inner corner of the eye. (3)The ocular features to
243 patients with COVID-19 mainly focuses on the inner and outer corner of the eye, the upper
244 and lower eyelid. (4)The model's features to patients with ocular diseases is mainly
245 focused on the iris and sclera, and the coverage is large and irregular. The convenience
246 and easy accedibility of the ocular photos based prediction would provide an alternative
247 setting for COVID-19 screening.

248 Meanwhile, there are some limits in this study. First, the study sample size is small and
249 most COVID-19 patients were collected from East Asia (China). A larger multicenter study
250 covering more patients with diverse race, would be necessary to test the performance of
251 the ocular surface feature based deep learning system. Secondly, the continuous
252 observations study covered only four COVID-19 patients with limited time points, and a

253 longitudinal observation study including more patients and time points would provide more
254 evidence to evaluate the screening performance of the model. As last, the pathological
255 significance of extracted features from COVID-19 patients should be carefully interpreted
256 and re-verified by ophthalmologist.
257

258 **Declarations**

259 **Authors' contributions**

260 Mengwei Gu (MG) and Feng Li (FL) conceived of the presented idea and discussed it with
261 others, and drafted the manuscript. Yanwei Fu (YF) and Xiangyang Xue (XX) contributed
262 to design the model, conducted experiments on all datasets and wrote the paper. Qiang
263 Sun (QS) and Haicheng Tang (HT) provided the major support to this work. Haicheng
264 Tang (HT) collected all data from the shanghai public health clinic center, and provided
265 medical guidance. Qiang Sun (QS) helped to improve the model. He also participated in
266 the paper writing. Xiangyang Xue revised the manuscript and supervised the project. All
267 authors provided critical feedback and helped shape the research, analysis, and
268 manuscript.

269

270 **Conflict of interest statements**

271 All other authors declare no competing interests.

272

273 **Ethics committee approval**

274 All participants were provided with written informed consent at the time of recruitment.
275 And this study was approved by the Ethics Committee of Shanghai public health clinic
276 center of Fudan University.

277

278

279

280

281

282

283 **Figure legends**

284 **Figure 1. Study design and workflow of this study.**

285 **Figure 2. Illustration of the modeling framework.**

286 **Figure 3. The ROC curves for the DL-based Classification Network in the**
287 **retrospective study.** The Model represents different validation subset for cross-validation.

288 **Figure 4. The ROC curves for the model to distinguish the (asymptomatic/mild)**
289 **COVID-19 patients to Healthy volunteers, Pulmonary and Ocular disease patients in**
290 **the prospective study.**

291

292

293 **Tables**

294 **Table 1. Summary of Training, Validation, and Testing Datasets.**

	Training & Validation		Testing	
	Subjects	Photos	Subjects	Photos
<i>Health</i>	143	447	35	162
<i>COVID-19</i>	104	367	29 (23 [*])	139 (99 [*])
<i>Pulmonary</i>	131	473	31	116
<i>Ocular</i>	68	274	33	130
<i>Total</i>	446	1561	128	547

295 * asymptomatic/mild.

296

297 **Table 2. The demographic and clinical characteristics of COVID-19 patients in this**
298 **study.**

	Retrospective(104)	Prospective(29)
Age, years	5-65 (100%)	20-59 (100%)
Sex		
Male	71(68.27%)	21(72.41%)
Female	33(31.73%)	8(27.59%)
Nationality		
East Asia	91(87.50%)	27(93.10%)
South Asia	10(9.62%)	0
Europe	2(1.92%)	2(6.90%)
South America	1(0.96%)	0
Other	0	0
Fever	35(33.65%)	8(27.59%)
Severity on admission		
asymptomatic/mild	24(23.08%)	23(79.31%)
Moderate	78(75.00%)	5(17.24%)
Severe	2(1.92%)	1(3.45%)

299

300 **Table 3. The 5-folder averaging classification performance of the DL-based model**
301 **on the training and validation datasets with one-vs.-rest and COVID-19-vs.-one**
302 **setting.**

Setting/Metric	AUC (95% CI)	Sensitivity (95% CI)	Specificity (95% CI)	ACC (95% CI)
One-vs.-Rest				
<i>Health vs. Rest</i>	0.983	0.871	0.955	0.930

	(0.971-0.994)	(0.803-0.983)	(0.928-0.983)	(0.901-0.959)
<i>COVID-19 vs. Rest</i>	0.999	0.982	0.978	0.979
	(0.997-1.000)	(0.954-1.000)	(0.961-0.995)	(0.963-0.994)
<i>Pulmonary vs. Rest</i>	0.969	0.853	0.941	0.915
	(0.950-0.988)	(0.784-0.922)	(0.911-0.971)	(0.884-0.945)
<i>Ocular vs. Rest</i>	0.986	0.846	0.972	0.949
	(0.976-0.995)	(0.749-0.942)	(0.954-0.989)	(0.926-0.973)
COVID-19-vs.-One				
<i>COVID-19 vs. Health</i>	0.999	0.998	0.967	0.979
	(0.998-1.000)	(0.993-1.000)	(0.944-0.990)	(0.965-0.993)
<i>COVID-19 vs. Pulmonary</i>	0.997	0.984	0.958	0.970
	(0.993-1.000)	(0.958-1.000)	(0.923-0.994)	(0.946-0.993)
<i>COVID-19 vs. Ocular</i>	1.000	1.000	0.989	0.995
	(1.000-1.000)	(1.000-1.000)	(0.977-1.000)	(0.989-1.000)

303

304 **Table 4. Classification Performance of the DL-based model on the testing datasets**

305 **with one vs. rest and one vs. one setting.**

Setting/Metric	AUC (95% CI)	Sensitivity (95% CI)	Specificity (95% CI)	ACC (95% CI)
One-vs.-Rest				
<i>Health vs. Rest</i>	0.930 (0.906-0.952)	0.926 (0.885-0.967)	0.740 (0.696-0.784)	0.795 (0.761-0.830)
<i>COVID-19 vs. Rest</i>	0.980 (0.970-0.990)	0.770 (0.694-0.846)	0.973 (0.957-0.989)	0.921 (0.898-0.945)
<i>Pulmonary vs. Rest</i>	0.869 (0.833-0.905)	0.440 (0.352-0.527)	0.940 (0.917-0.963)	0.834 (0.802-0.865)
<i>Ocular vs. Rest</i>	0.968 (0.953-0.983)	0.762 (0.687-0.836)	0.993 (0.984-1.000)	0.938 (0.917-0.958)
COVID-19-vs.-One				
<i>COVID-19 vs. Health</i>	0.963 (0.944-0.982)	0.784 (0.714-0.854)	0.938 (0.901-0.975)	0.867 (0.829-0.905)
<i>COVID-19 vs. Pulmonary</i>	1.000 (1.000-1.000)	0.971 (0.943-1.000)	1.000 (1.000)	0.984 (0.969-1.000)
<i>COVID-19 vs. Ocular</i>	0.998 (0.996-1.000)	0.957 (0.923-0.991)	0.992 (0.977-1.000)	0.974 (0.955-1.993)
COVID-19 (asymptomatic/mild)-vs.-One				
<i>COVID-19 vs. Health</i>	0.960	0.757	0.938	0.868

	(0.939-9.981)	(0.675-0.840)	(0.901-0.975)	(0.827-0.909)
<i>COVID-19 vs. Pulmonary</i>	1.000	0.990	1.000	0.995
	(1.000-1.000)	(0.971-1.00)	(1.000-1.000)	(0.986-1.000)
<i>COVID-19 vs. Ocular</i>	0.999	0.971	0.992	0.983
	(0.997-1.000)	(0.938-1.000)	(0.977-1.000)	(0.966-1.000)

306

307 **Table 5. The confusion matrix of classification result of subjects into the**
308 **retrospective and prospective study.**

GT/Predict	Prospective study				Retrospective study			
	Health	COVID	Pulmonary	Ocular	Health	COVID	Pulmonary	Ocular
Health	150	10	0	2	27	6	0	2
COVID-19	30	107	2	0	1	28	0	0
Pulmonary	64	0	51	1	7	0	23	1
Ocular	6	1	24	99	0	1	8	24

309

310

311 **Table 6. The ablation study on using full eyes, left eye and right eye in the**
312 **retrospective training and validation dataset.**

Setting/Metric	AUC (95% CI)	Sensitivity (95% CI)	Specificity (95% CI)	ACC (95% CI)
One-vs.-Rest (full)				
<i>Health vs. Rest</i>	0.983 (0.971-0.994)	0.871 (0.803-0.983)	0.955 (0.928-0.983)	0.930 (0.901-0.959)
<i>COVID-19 vs. Rest</i>	0.999 (0.997-1.000)	0.982 (0.954-1.000)	0.978 (0.961-0.995)	0.979 (0.963-0.994)
<i>Pulmonary vs. Rest</i>	0.969 (0.950-0.988)	0.853 (0.784-0.922)	0.941 (0.911-0.971)	0.915 (0.884-0.945)
<i>Ocular vs. Rest</i>	0.986 (0.976-0.995)	0.846 (0.749-0.942)	0.972 (0.954-0.989)	0.949 (0.926-0.973)
One-vs.-Rest (left)				
<i>Health vs. Rest</i>	0.984 (0.971-0.996)	0.900 (0.837-0.962)	0.954 (0.926-0.982)	0.939 (0.912-0.966)
<i>COVID-19 vs. Rest</i>	0.999 (0.997-1.000)	0.976 (0.950-1.000)	0.974 (0.955-0.992)	0.974 (0.956-0.992)
<i>Pulmonary vs. Rest</i>	0.969 (0.951-0.986)	0.859 (0.789-0.929)	0.920 (0.884-0.956)	0.902 (0.868-0.935)
<i>Ocular vs. Rest</i>	0.977 (0.962-0.993)	0.741 (0.625-0.856)	0.983 (0.968-0.997)	0.940 (0.913-0.966)
One-vs.-Rest (right)				

<i>Health vs. Rest</i>	0.989 (0.981-0.997)	0.920 (0.865-0.975)	0.963 (0.939-0.988)	0.951 (0.927-0.975)
<i>COVID-19 vs. Rest</i>	0.999 (0.997-1.000)	0.981 (0.950-1.000)	0.989 (0.976-1.000)	0.987 (0.974-0.999)
<i>Pulmonary vs. Rest</i>	0.974 (0.955-0.992)	0.895 (0.837-0.954)	0.942 (0.910-0.973)	0.927 (0.898-0.957)
<i>Ocular vs. Rest</i>	0.982 (0.968-0.996)	0.802 (0.694-0.911)	0.978 (0.960-0.995)	0.947 (0.922-0.972)

313

314

315 **Table 7. The continuous observations of patients who turn into COVID-19 negative.**

Patients/Batch	First (Positive)			Second (Negative)		
	Positive	Negative	Date	Positive	Negative	Date
<i>C004</i>	4	0	2020-09-07	3	1	2020-09-10
<i>C011</i>	3	1	2020-09-07	3	1	2020-09-10
<i>C037</i>	3	1	2020-09-08	1	2	2020-09-12
<i>C039</i>	2	2	2020-09-08	1	3	2020-09-12
<i>Total</i>	12	4		8	7	

316

317

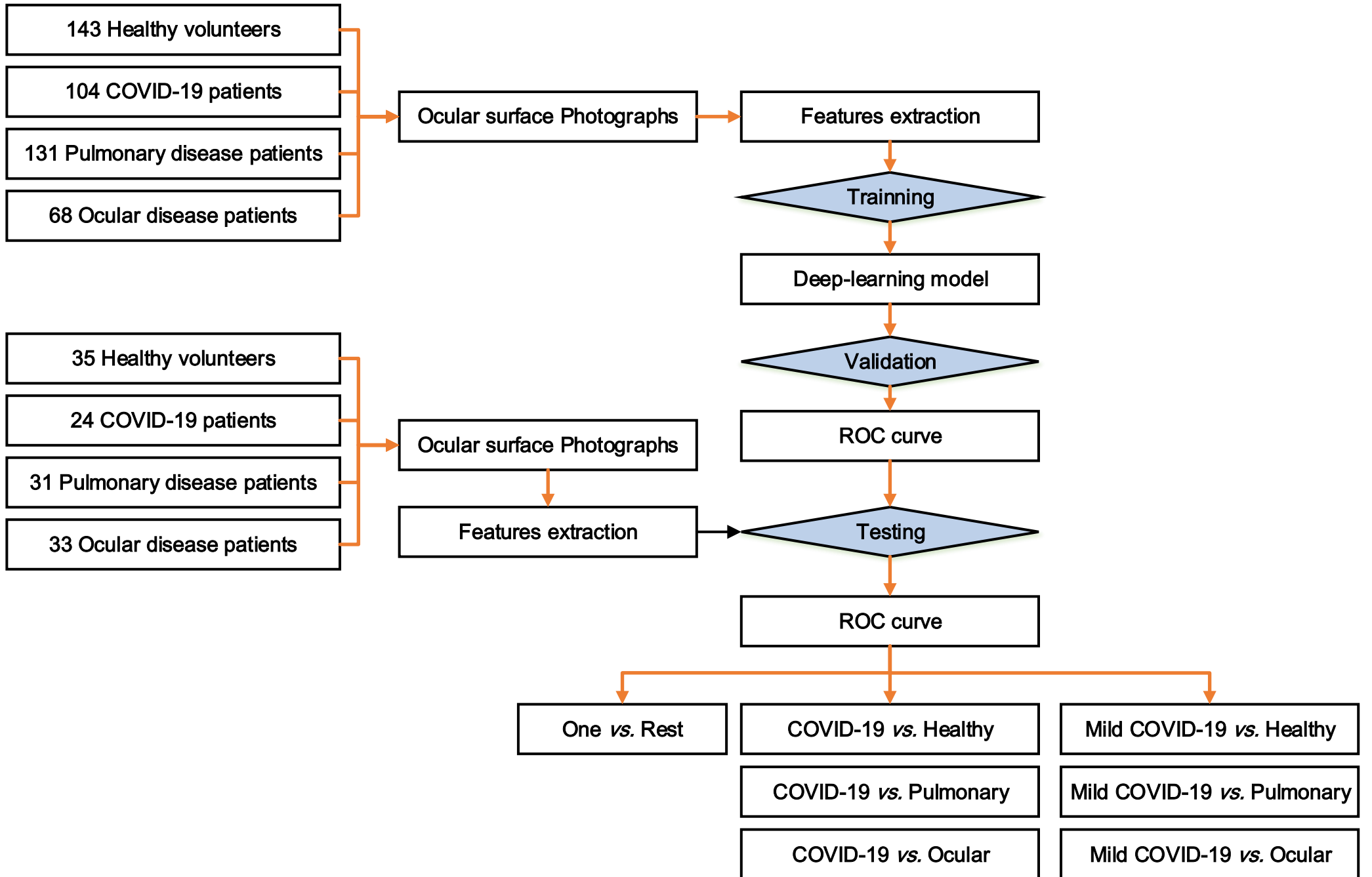
318

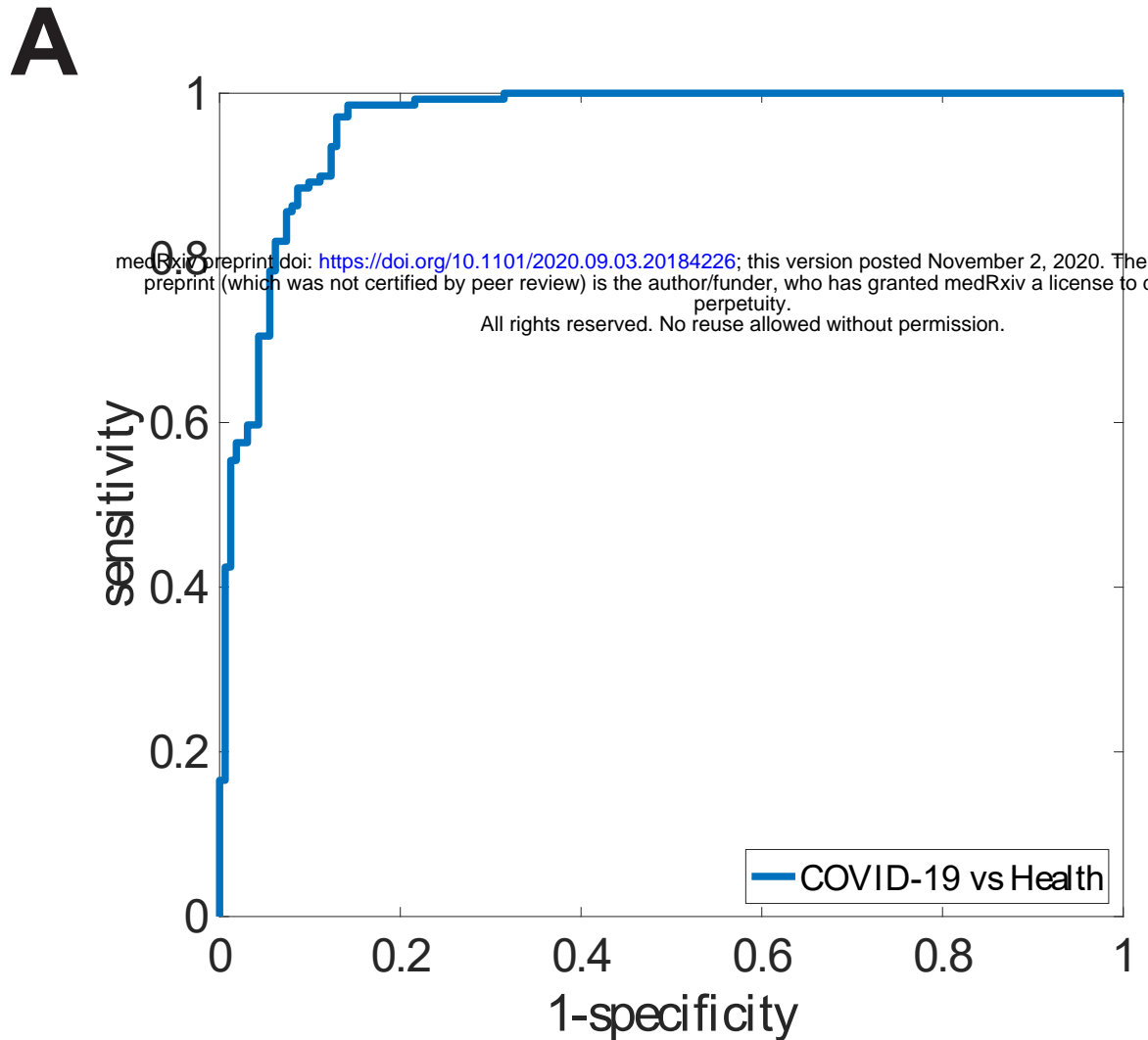
319

320

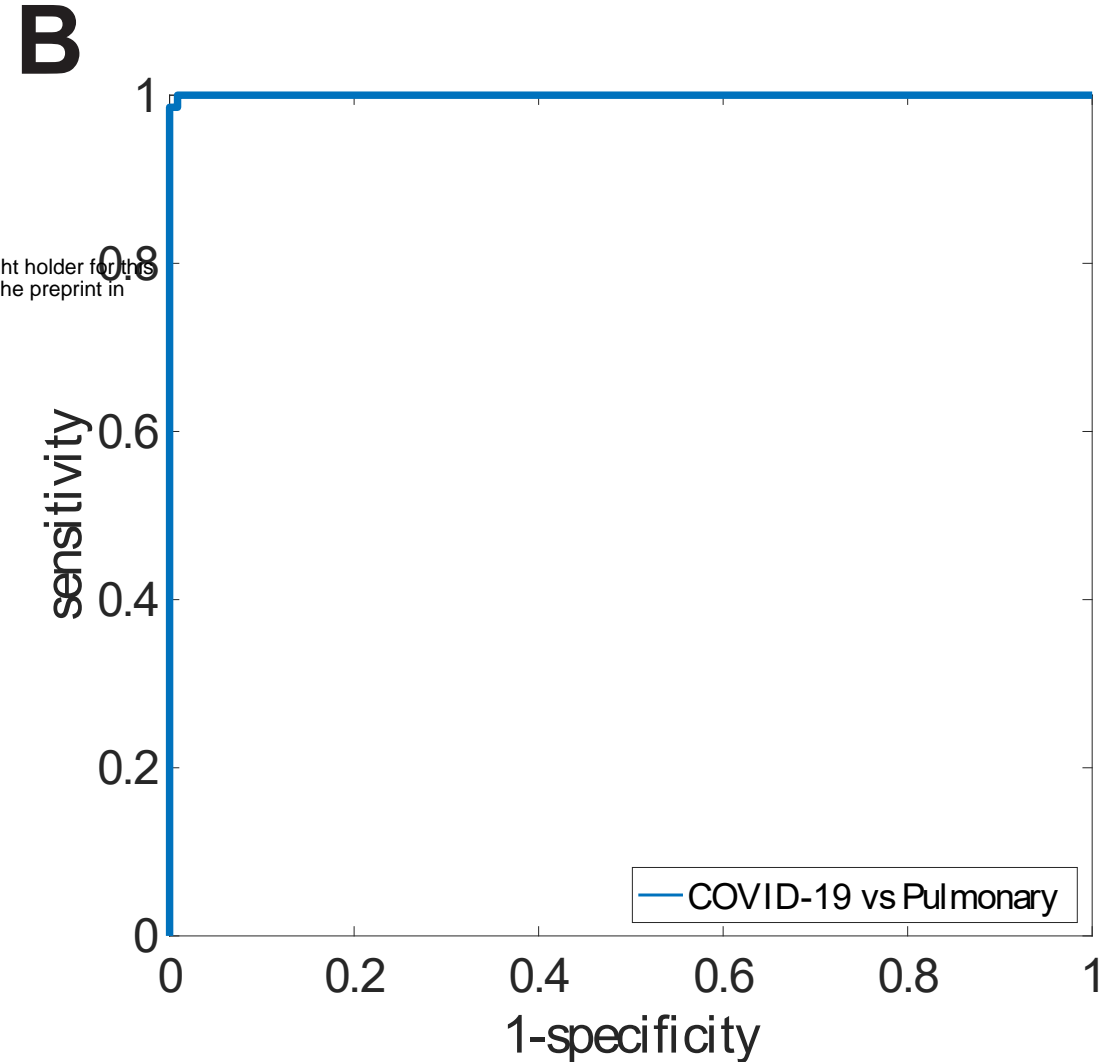
321 **Reference**

- 322 1. Rodriguez Mega, E. COVID has killed more than one million people. How many more will
323 die? *Nature* (2020).
- 324 2. Guan, W.J., *et al.* Clinical Characteristics of Coronavirus Disease 2019 in China. *N Engl J*
325 *Med* **382**, 1708-1720 (2020).
- 326 3. Huang, C., *et al.* Clinical features of patients infected with 2019 novel coronavirus in
327 Wuhan, China. *Lancet* **395**, 497-506 (2020).
- 328 4. Wang, D., *et al.* Clinical Characteristics of 138 Hospitalized Patients With 2019 Novel
329 Coronavirus-Infected Pneumonia in Wuhan, China. *JAMA* **323**, 1061-1069 (2020).
- 330 5. Wynants, L., *et al.* Prediction models for diagnosis and prognosis of covid-19 infection:
331 systematic review and critical appraisal. *BMJ* **369**, m1328 (2020).
- 332 6. Long, Q.X., *et al.* Clinical and immunological assessment of asymptomatic SARS-CoV-2
333 infections. *Nat Med* **26**, 1200-1204 (2020).
- 334 7. Mei, X., *et al.* Artificial intelligence-enabled rapid diagnosis of patients with COVID-19.
335 *Nat Med* **26**, 1224-1228 (2020).
- 336 8. Zhang, K., *et al.* Clinically Applicable AI System for Accurate Diagnosis, Quantitative
337 Measurements, and Prognosis of COVID-19 Pneumonia Using Computed Tomography.
338 *Cell* **181**, 1423-1433 e1411 (2020).
- 339 9. Ting, D.S.W., *et al.* Development and Validation of a Deep Learning System for Diabetic
340 Retinopathy and Related Eye Diseases Using Retinal Images From Multiethnic
341 Populations With Diabetes. *JAMA* **318**, 2211-2223 (2017).
- 342 10. Colavita, F., *et al.* SARS-CoV-2 Isolation From Ocular Secretions of a Patient With
343 COVID-19 in Italy With Prolonged Viral RNA Detection. *Ann Intern Med* **173**, 242-243
344 (2020).
- 345 11. Gupta, A., *et al.* Extrapulmonary manifestations of COVID-19. *Nat Med* **26**, 1017-1032
346 (2020).
- 347 12. Kirschenbaum, D., *et al.* Inflammatory olfactory neuropathy in two patients with
348 COVID-19. *Lancet* **396**, 166 (2020).
- 349 13. Zhou, Y., *et al.* Ocular Findings and Proportion with Conjunctival SARS-COV-2 in
350 COVID-19 Patients. *Ophthalmology* **127**, 982-983 (2020).
- 351 14. T Wang, J.C., A Hunter, D Greig. Learnable Stroke Models for Example-based Portrait
352 Painting. *BMVC* (2013).
- 353 15. A Krizhevsky, I.S., GE Hinton. Imagenet classification with deep convolutional neural
354 networks. *Advances in Neural Information Processing Systems 25 (NIPS 2012)* (2012).
- 355 16. Simonyan, K., and Andrew Zisserman. Very Deep Convolutional Networks for
356 Large-Scale Image Recognition. *ICLR 2015: International Conference on Learning*
357 *Representations* (2015).
- 358 17. Huang, P.W. & Lee, C.H. Automatic classification for pathological prostate images based
359 on fractal analysis. *IEEE Trans Med Imaging* **28**, 1037-1050 (2009).
- 360 18. Zia, M.S., Majid Hussain, and M. Arfan Jaffar. A novel spontaneous facial expression
361 recognition using dynamically weighted majority voting based ensemble classifier.
362 *Multimedia Tools and Applications* (2018).
- 363

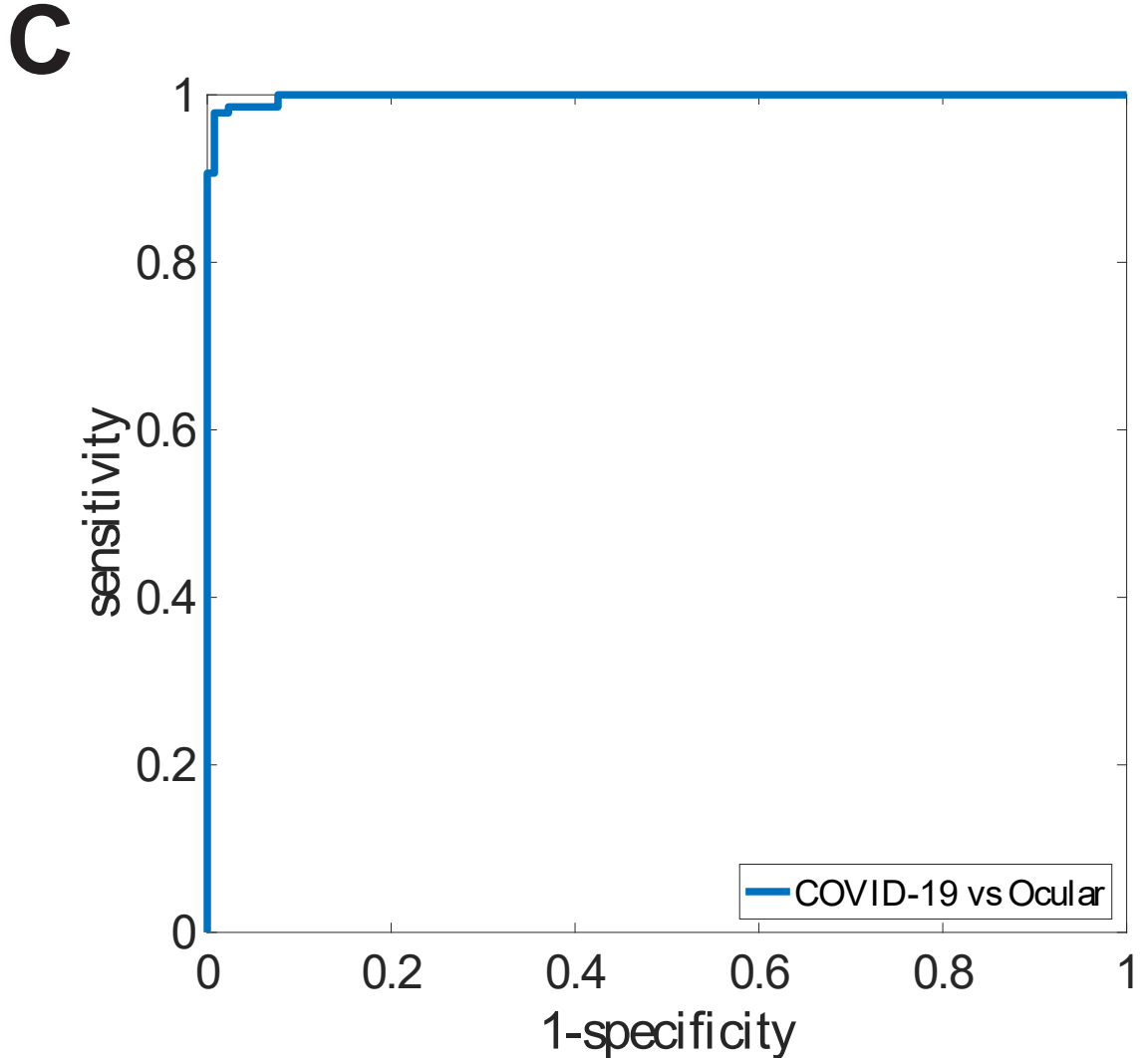




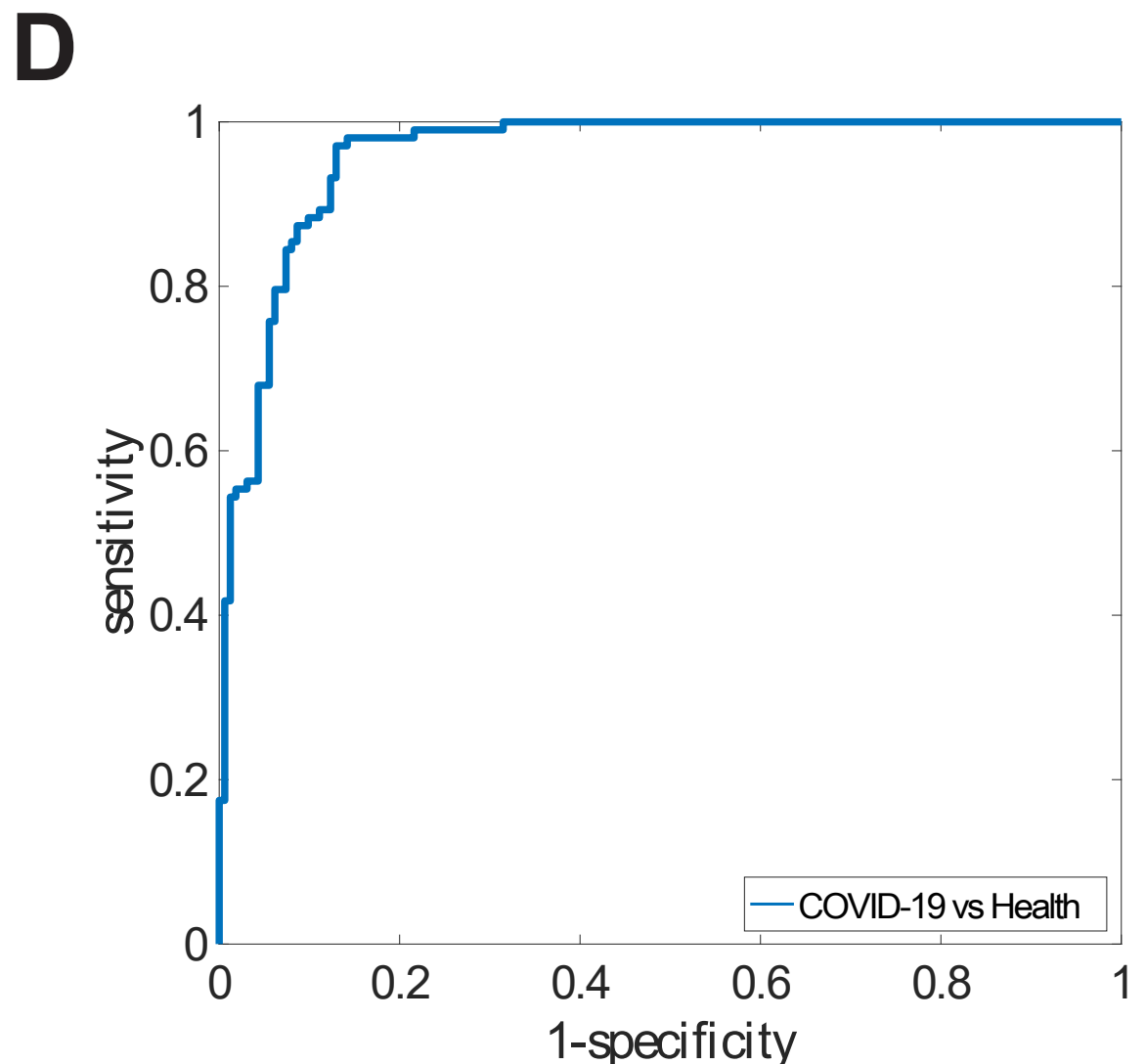
COVID-19 vs healthy volunteer



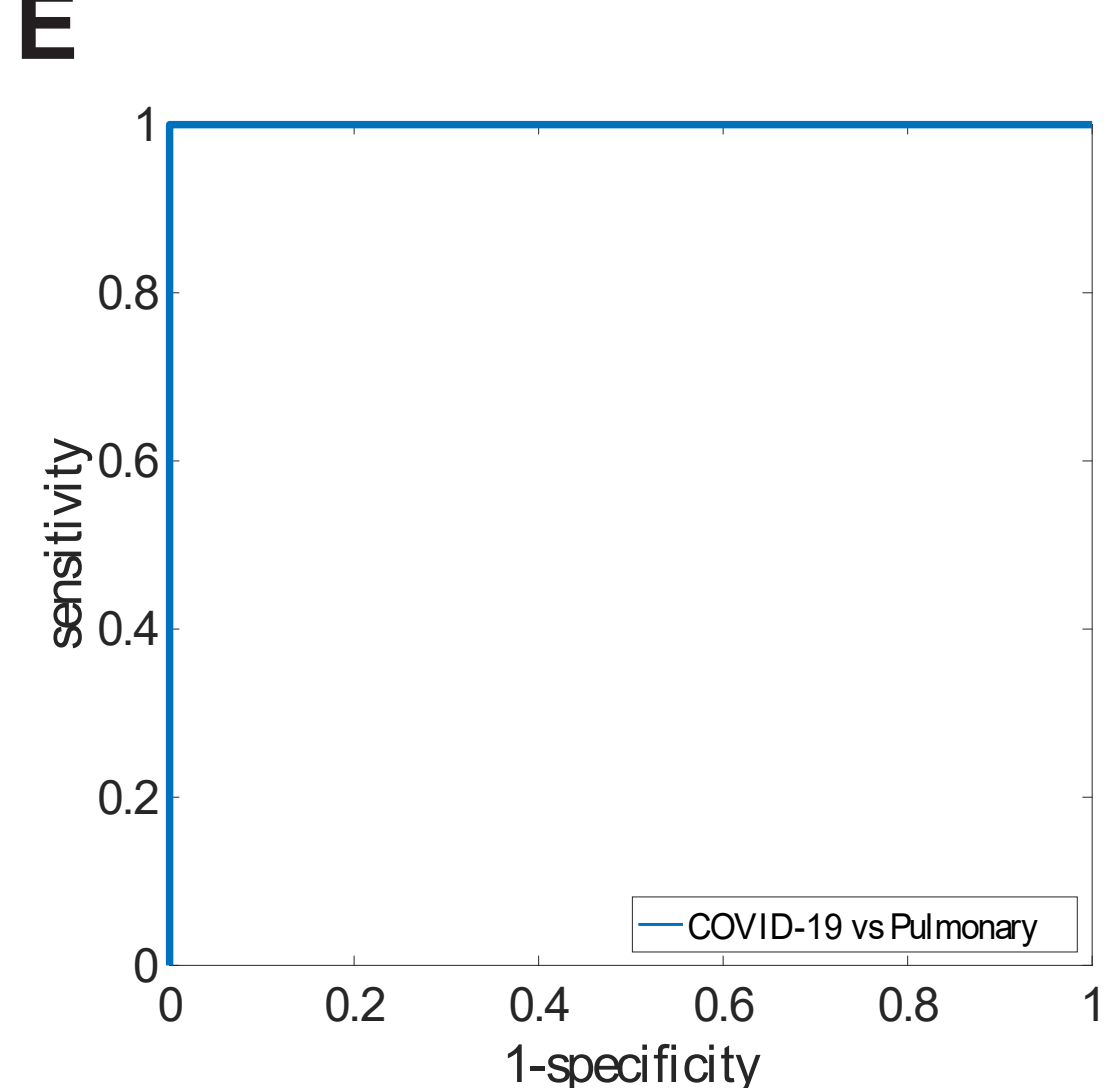
COVID-19 vs Pulmonary disease



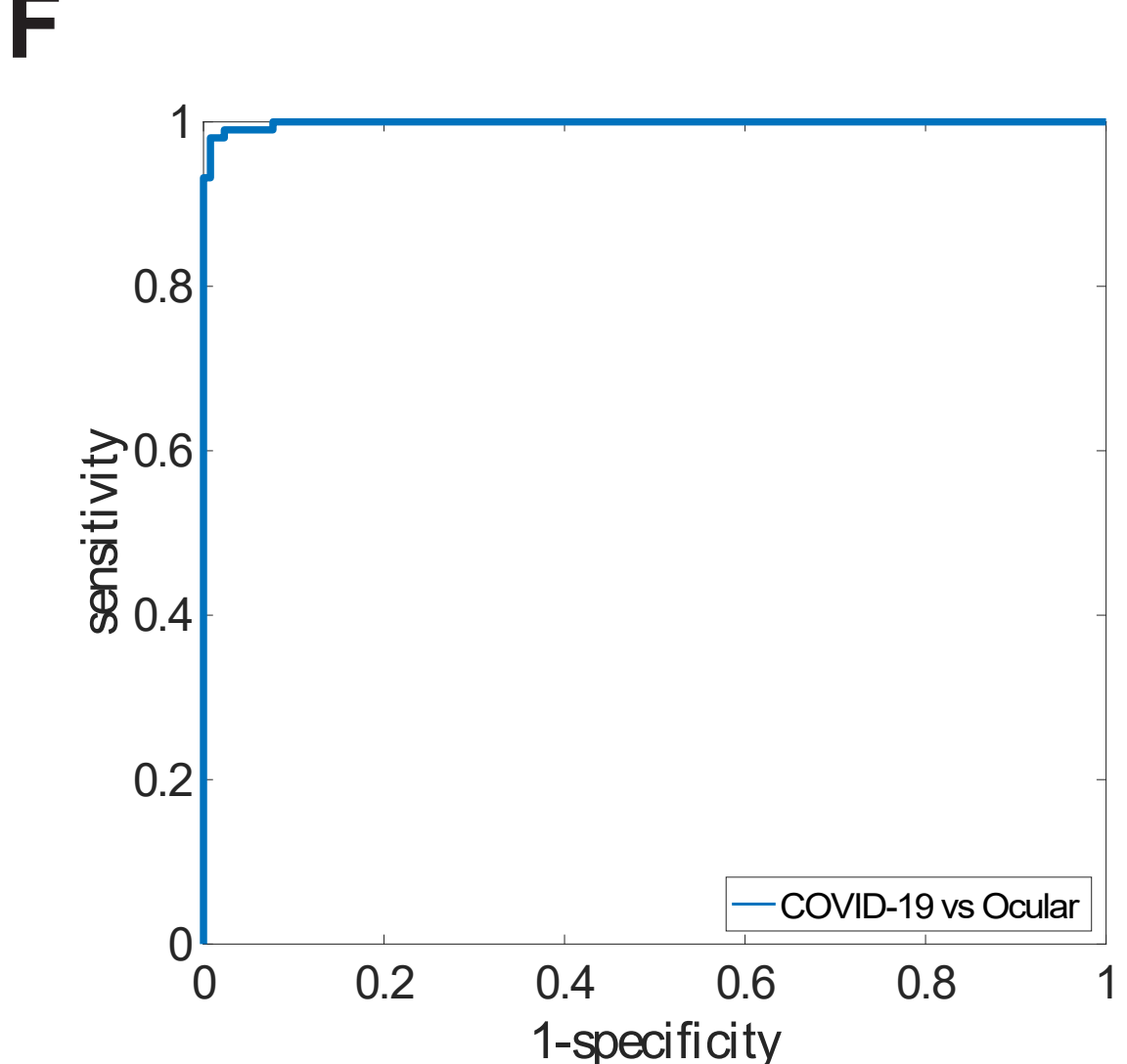
COVID-19 vs Ocular disease



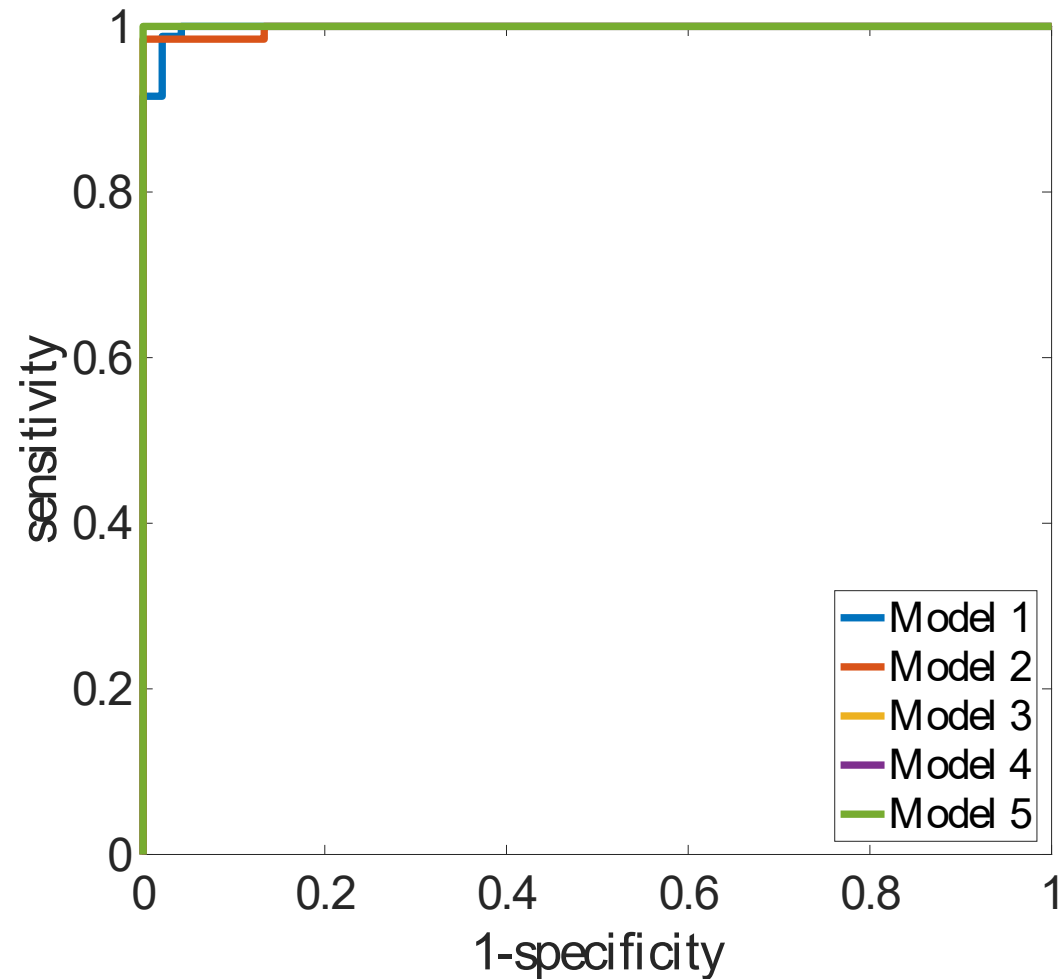
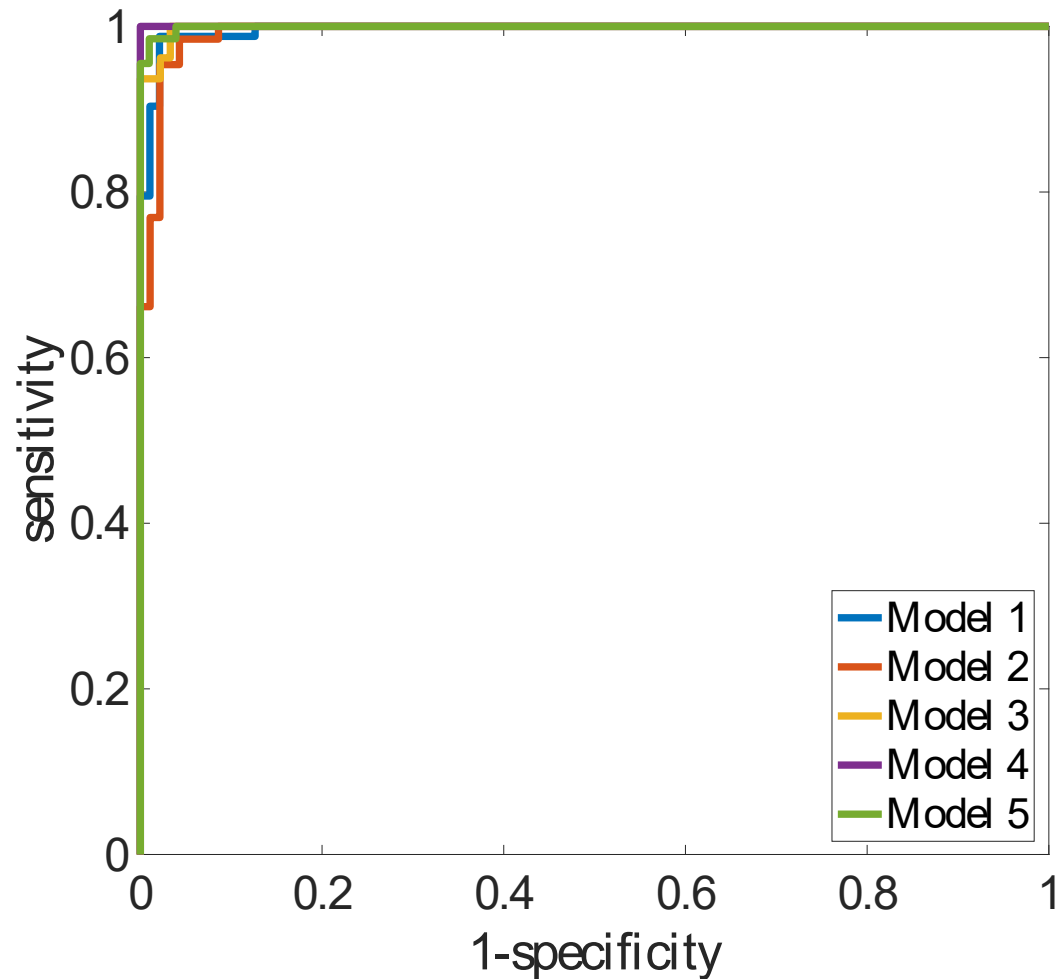
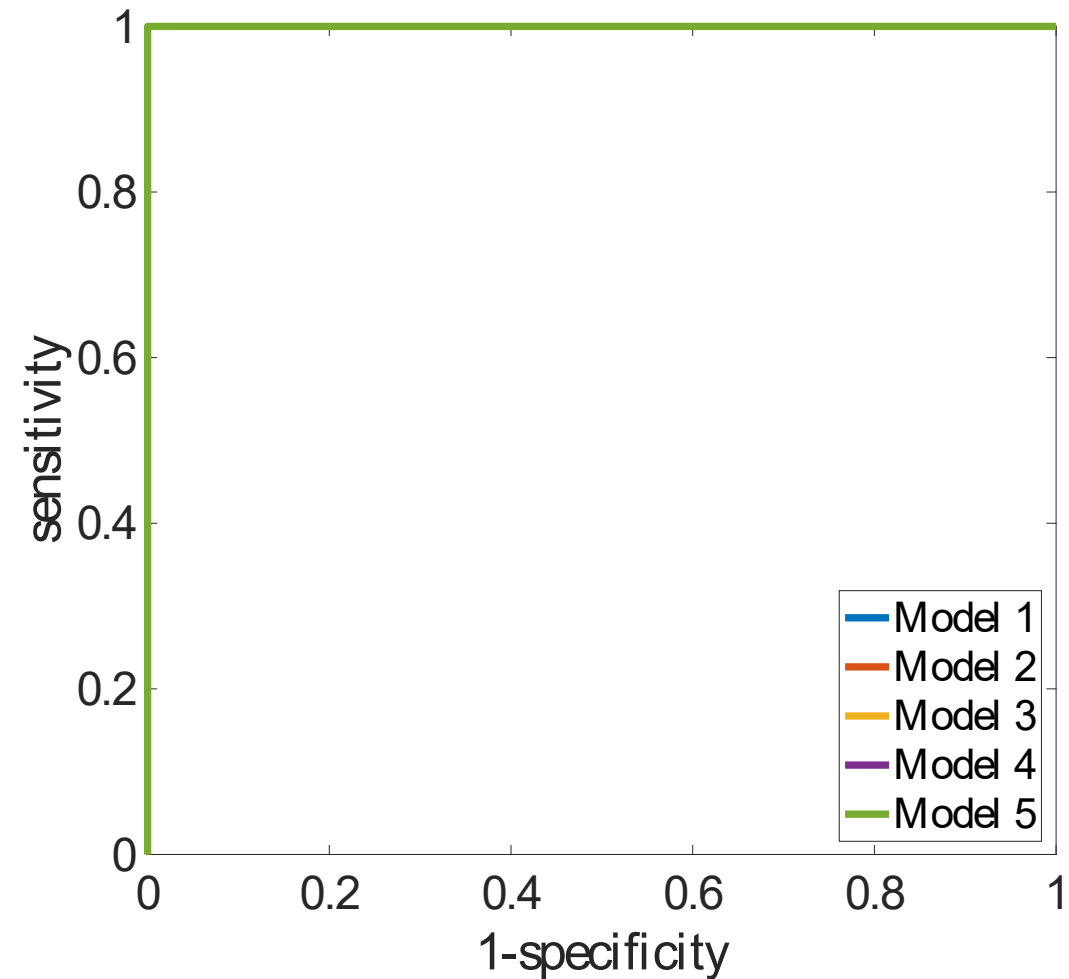
Mild COVID-19 vs healthy volunteer



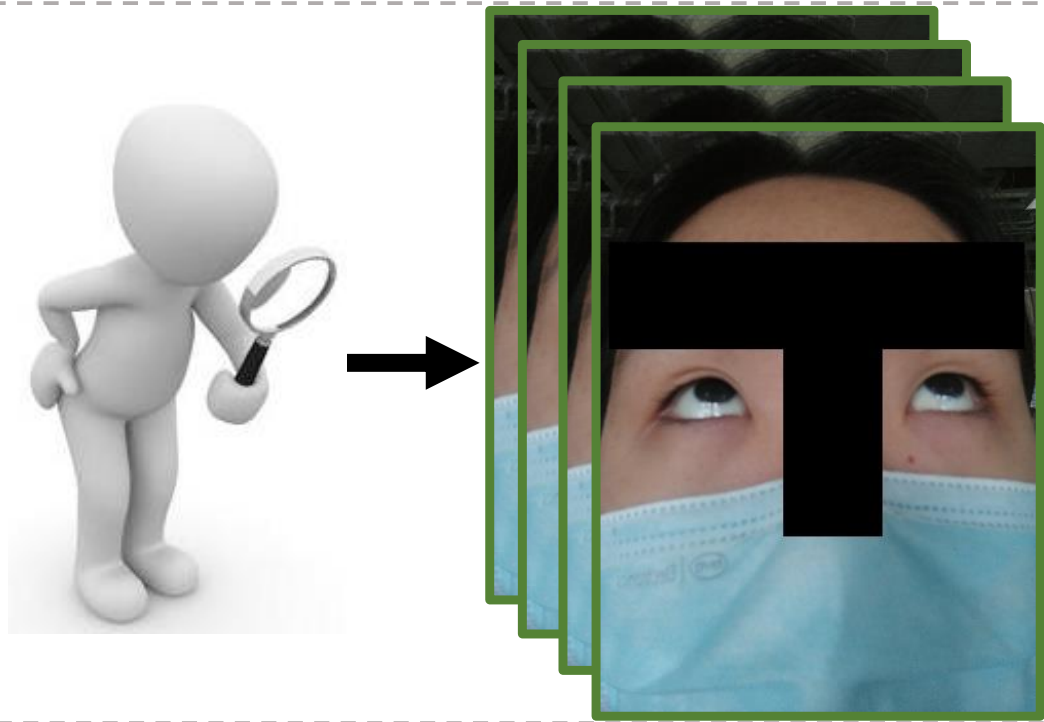
Mild COVID-19 vs Pulmonary disease



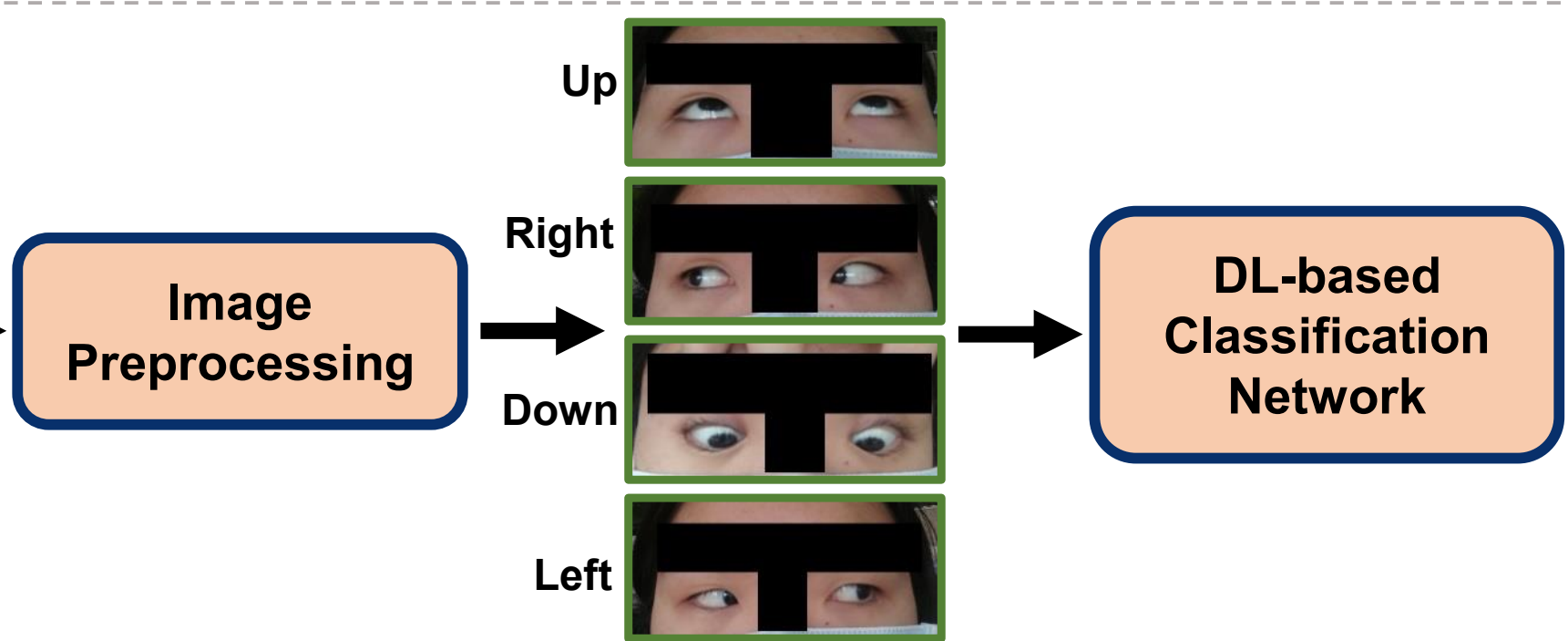
Mild COVID-19 vs Ocular disease

A**COVID-19 vs healthy volunteer****B****COVID-19 vs Pulmonary disease****C****COVID-19 vs Ocular disease**

Input



Model



Output

